

Paired Wasserstein Autoencoders for Conditional Sampling

Moritz Piening¹[0009-0003-3877-4511] and Matthias Chung²[0000-0001-7822-4539]

¹ Technical University of Berlin, Berlin, Germany piening@math.tu-berlin.de

² Emory University, Atlanta, GA, USA matthiaschung@emory.edu

Abstract. Wasserstein distances greatly influenced and coined various types of generative neural network models. Wasserstein autoencoders are particularly notable for their mathematical simplicity and straightforward implementation. However, their adaptation to the conditional case displays theoretical difficulties. As a remedy, we propose the use of two paired autoencoders. Under the assumption of an optimal autoencoder pair, we leverage the pairwise independence condition of our prescribed Gaussian latent distribution to overcome this theoretical hurdle. We conduct several experiments to showcase the practical applicability of the resulting paired Wasserstein autoencoders. Here, we consider imaging tasks and enable conditional sampling for denoising, inpainting, and unsupervised image translation. Moreover, we connect our image translation model to the Monge map behind Wasserstein-2 distances.

Keywords: Wasserstein autoencoders · Conditional generative model · Image reconstruction · Uncertainty quantification · Inverse problems

1 Introduction

Uncertainty quantification, essential in imaging applications, is often framed within Bayesian inference [24]. This approach reconstructs a conditional distribution using neural networks to model the probability of the true image given observed data, enabling both image estimation and uncertainty quantification. Such methods are critical in medical and scientific contexts, where confidence in reconstructed images informs decision-making. Advances in deep learning, particularly conditional generative models, have facilitated uncertainty integration in image reconstruction. These models are typically trained using paired data [10], variational frameworks [21], supervised learning with data fidelity [23], or joint distribution assumptions for unpaired samples [17]. Among the various generative neural network models, we consider Wasserstein autoencoders due to their intuitive nature and the usefulness of the induced latent embedding [25]. These models have been motivated by optimal transport, especially Wasserstein distances. While Wasserstein autoencoders enable unconditional sampling, conditional adaptations are crucial for generative modeling. Despite successful adaptation to the conditional case [9,14,15], the theoretical underpinning remains unclear because Wasserstein upper bounds on the unconditional distribution do

not imply conditional upper bounds [3] and model dependence on the condition respectively the observed data is not ensured [14]. In this work, we aim to construct conditional Wasserstein autoencoders that allow for conditional sampling with a theoretical background. To this end, we utilize paired autoencoders and prescribe the latent distribution to resemble an isotropic Gaussian. Assuming a set of optimal autoencoders, we can make use of the pairwise independence of normal variables to generate conditional samples.

This work is organized as follows. In Section 2, we provide the necessary background on conditional generative models, optimal transport, and autoencoders. Section 3 introduces our proposed method, paired Wasserstein autoencoders, see Fig. 1. In Section 4, we present experiments to support our approach. Finally, we conclude our investigation with a brief discussion in Section 5.

2 Background

In this section, we give an overview of relevant related work and introduce basic concepts for our paired Wasserstein autoencoder framework.

Conditional Generative Models. In the past decade, generative modeling has had tremendous success in imaging. Notable examples include generative adversarial networks [7], generative autoencoders [25], diffusion models [12], gradient flow models [11] and flow matching models [19]. In addition to unconditional sampling from data distributions, these models can be extended to facilitate conditional sampling, as demonstrated in [1,3,10]. Here, we aim to reconstruct the conditional distribution of the random variable $(X_1|X_2 = x_2)$ characterized by the probability measure $\mu_{X_1|X_2=x_2}$. Conditional generative modeling aims to learn a neural network $T^\theta: \mathbb{R}^{d_1} \times \mathbb{R}^{d_2} \rightarrow \mathbb{R}^{d_3}$ that maps a d_1 -dimensional latent distribution μ_Z to the conditional distribution $\mu_{X_1|X_2=x_2}$. This is achieved by ensuring that the conditional distribution satisfies

$$\mu_{X_1|X_2=x_2} = (T^\theta(\cdot, x_2))\#\mu_Z,$$

where $(T^\theta(\cdot, x_2))\#\mu_Z$ denotes the pushforward of μ_Z through the mapping $T^\theta(\cdot, x_2)$. Intuitively, the network learns to transform samples from the latent distribution μ_Z into samples from $\mu_{X_1|X_2=x_2}$ conditioned on x_2 . Specifically, for any measurable set $\mathcal{A} \subseteq \mathcal{X}$, the relationship can be expressed as

$$\mu_{X_1|X_2=x_2}(\mathcal{A}) = \mu_Z((T^\theta)^{-1}(\mathcal{A}, x_2)),$$

where $(T^\theta)^{-1}(\mathcal{A}, x_2) = \{z \in \mathcal{Z} : T^\theta(z, x_2) \in \mathcal{A}\}$.

Being able to sample from the learned distribution, allows for insights into statistical properties, such as the mean and standard deviation, as a tool for uncertainty quantification. Such conditional sampling has important applications in, e.g., Bayesian inverse problems [21] and unsupervised image translation [17]. Despite impressive results, many conditional models rely on invertible networks

[2] with limited expressiveness or computationally costly time-continuous transformations [8]. Moreover, many conditional models employed for inverse problems often work without the data fidelity term, e.g., [10]. Research on uncertainty quantification with combinations of generative modeling and data fidelity terms exists, e.g., [4,23], but remains limited for now and often relies on costly optimization procedures. To allow for single-step posterior sampling with a data fidelity term and unrestricted neural networks, we combine ideas from the existing work on paired neural networks [6], generative models based on shared latent spaces [13], and conditional Wasserstein autoencoders [9,14,15].

Measure Couplings & Optimal Transport. The field of optimal transport has greatly impacted machine learning and generative modeling, e.g., [3,17,21]. In particular, Wasserstein distances enable comparison between probability measures based on optimal transport theory. To draw on this theory, we give an overview of related concepts. Consider random variables (X_1, \dots, X_N) governed by probability measures $(\mu_{X_1}, \dots, \mu_{X_N})$, where μ_{X_i} has support $\text{supp}(\mu_{X_i}) = \mathcal{X}_i \subset \mathbb{R}^{d_i}$. The set of all (multi-marginal) couplings of these measures is

$$\Pi(\mu_{X_1}, \dots, \mu_{X_N}) = \left\{ \pi \in \mathcal{P} \left(\prod_{i=1}^N \mathcal{X}_i \right) \mid \text{Proj}_{X_i} \pi = \mu_{X_i}, \forall i \right\}.$$

Here, $\mathcal{P}(\prod_{i=1}^N \mathcal{X}_i)$ is the space of probability measures on the product space $\prod_{i=1}^N \mathcal{X}_i$, and Proj_{X_i} denotes the projection onto the X_i -component. Specifically, for a measure π on $\prod_{i=1}^N \mathcal{X}_i$, the projection $\text{Proj}_{X_i} \pi$ is the marginal distribution of π on \mathcal{X}_i , defined by

$$\text{Proj}_{X_i} \pi(B) = \pi \left(\left\{ x \in \prod_{j=1}^N \mathcal{X}_j \mid x_i \in B \right\} \right)$$

for any measurable set $B \subseteq \mathcal{X}_i$. Then, the Wasserstein- p distance between two random variables $X_1 \sim \mu_{X_1}, X_2 \sim \mu_{X_2} \in \mathcal{P}(\mathcal{X})$ with $\mathcal{X} \subset \mathbb{R}^d$ is defined as

$$W_p^p(X_1, X_2) := \inf_{\pi \in \Pi(\mu_{X_1}, \mu_{X_2})} \mathbb{E}_{(X_1, X_2) \sim \pi} \|X_1 - X_2\|_p^p. \quad (1)$$

This distance is a metric on the space of real-valued probability measures with finite p -th moment. Furthermore, under certain regularity conditions, the optimal transport plan for the Wasserstein-2 distance is realized as a (unique) deterministic transport map. This means that there exists exactly one map $T : \mathcal{X} \rightarrow \mathcal{X}$, such that the optimizer in (1) fulfills $\pi^* = (\mu_{X_1}, T_{\#} \mu_{X_1})$ with

$$W_2^2(X_1, X_2) = \mathbb{E}_{X_1 \sim \mu_{X_1}} \|X_1 - T(X_1)\|_2^2.$$

This map is known as the *Monge map*. For a detailed background on optimal transport theory, we refer the interested reader to [22]. This theory has led to fruitful applications in generative modeling [17,21,25] which we want to explore further. In particular, we aim to overcome the theoretical challenges of adapting Wasserstein distances to conditional modeling, see [3] for an in-depth discussion.

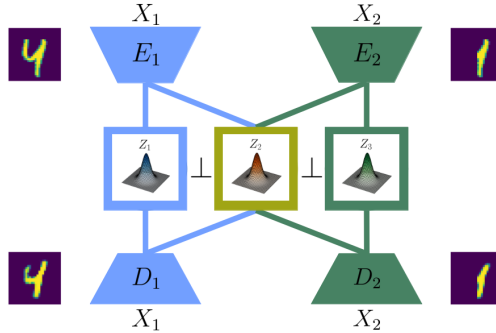


Fig. 1: Our paired Wasserstein autoencoder consists of two paired autoencoders composed of encoder E_1 and decoder D_1 (blue) and E_2 and D_2 (green) respectively mapping images X_1 and X_2 from two different distributions to a partially shared latent distribution $Z = (Z_1, Z_2, Z_3)$ (blue, yellow, green) described by a standard Gaussian. Due to the pairwise independence of the latent variables denoted by \perp , we can approximate conditional samples of $(X_1|X_2 = x_2)$. The example shows inpainting with full image X_1 and masked image X_2 .

3 Paired Wasserstein-Autoencoders for Conditional Sampling

We consider *implicit* generative models [25] based on a latent space. In this setting, a latent variable Z is sampled from a predefined probability measure μ_Z on a space \mathcal{Z} . Generally, we consider μ_Z to be standard Gaussian in the latent space. After sampling, the latent variable Z is mapped to $D(Z) \in \mathcal{X} \subset \mathbb{R}^d$ by a decoder $D: \mathcal{Z} \rightarrow \mathcal{X}$. This leads to latent variable models with probability measures μ_Y defined on \mathcal{X} . In this setting, a latent variable Z is sampled from a predefined probability measure μ_Z on a space \mathcal{Z} . Typically, μ_Z is chosen as the standard Gaussian measure in the latent space. The latent variable Z is then mapped to a point $D(Z) \in \mathcal{X} \subset \mathbb{R}^d$ by a decoder $D: \mathcal{Z} \rightarrow \mathcal{X}$. This induces a pushforward measure μ_Y on \mathcal{X} via the decoder D , specifically,

$$\mu_Y = D\#\mu_Z.$$

For a deterministic decoder D , this simplifies: D maps each $z \in \mathcal{Z}$ to a single point in \mathcal{X} . Here, μ_Y is the pushforward of μ_Z and is given by:

$$\mu_Y(A) = \mu_Z(D^{-1}(A)), \quad \text{for any measurable } A \subseteq \mathcal{X}, \quad (2)$$

where $D^{-1}(A) = \{z \in \mathcal{Z} \mid D(z) \in A\}$ is the preimage of A under D .

Wasserstein Autoencoders. Wasserstein autoencoders are fundamental generative models using encoder-decoder architectures, where the encoder-induced latent distribution is aligned with a predefined one, typically Gaussian. Unlike variational autoencoders, which use the Kullback-Leibler divergence, Wasserstein autoencoders are based on optimal transport theory. Indeed, they approximate the Wasserstein distance between a reference distribution and a lower-dimensional representation of the target distribution, shown in [25]:

Theorem 1. *Given continuous measures $\mu_X, \mu_Y \in \mathcal{P}(\mathcal{X})$ and $\mu_Z \in \mathcal{P}(\mathcal{Z})$ with $Y \sim \mu_Y$ characterized by (2) and $(Y|Z = z) \sim \mu_{Y|Z=z} = \delta_{D(z)}$ for some function $D: \mathcal{Z} \rightarrow \mathcal{X}$, we have*

$$\begin{aligned} W_p^p(X, Y) &= \inf_{\pi \in \Pi(\mu_X, \mu_Z)} \mathbb{E}_{(X, Z) \sim \pi} \|X - D(Z)\|_p^p \\ &= \inf_{\pi \in \Pi(\mu_X, \mu_Z)} \mathbb{E}_{\mu_X} \mathbb{E}_{E_{Z|X}^\pi} \|X - D(Z)\|_p^p, \end{aligned}$$

where $E_{Z|X}^\pi := \text{Proj}_{Z|X} \pi$ is the probability measure of the conditional marginal distribution of the optimal coupling.

We view $E_{Z|X}^\pi$ as a non-deterministic map that maps X to Z . Theorem 1 states that, we can directly minimize couplings between the reference and the latent distributions instead of couplings between the reference and the target distribution. Theoretically, we can minimize the Wasserstein distance between the reference distribution and the one generated by the decoder by alternating optimization of the encoder and decoder, fixing one while optimizing the other. For practical applications, this means that we can parameterize an encoder $E^\theta: \mathcal{X} \rightarrow \mathcal{Z}$ and a decoder $D^\theta: \mathcal{Z} \rightarrow \mathcal{X}$ using neural networks and minimize the cost functional under the constraints on the marginals. If the cost vanishes and the latent constraints are fulfilled, the Wasserstein distance between the reference distribution and the generated target one vanishes. In practice, empirical distributions, mini-batches, and relaxation enable model training. Unconditional samples are obtained by passing latent Gaussian variables through the decoder.

Conditional Adaptation. The standard Wasserstein autoencoder does not enable sampling from a distribution conditioned on an observation. Nevertheless, this is often desirable for practical applications of generative modeling. Extensions of the Wasserstein autoencoder to the conditional case exist, but their losses only bound unconditional Wasserstein distances [3,15] and do not directly enforce the impact of the condition [14]. Ensuring the unconditional latent distribution to be Gaussian does not guarantee the conditional latent distribution to be Gaussian. As a result, we want to investigate the question of conditioning Wasserstein autoencoders through a set of paired autoencoders. A pair of optimal decoders could perfectly reconstruct the distribution of the conditional variable and the conditioned variable. We start with observing some theoretical properties of such a pair of optimal decoders. Here, we use \perp to denote (conditional) independence.

Proposition 1. *Let $X = (X_1, X_2) \in \mathcal{X} = \mathcal{X}_1 \times \mathcal{X}_2 \subset \mathbb{R}^{d_1} \times \mathbb{R}^{d_2}$ and $D = (D_1, D_2)$, where $D_1: \mathcal{Z}_1 \times \mathcal{Z}_2 \rightarrow \mathcal{X}_1$ and $D_2: \mathcal{Z}_2 \times \mathcal{Z}_3 \rightarrow \mathcal{X}_2$ for $\mathcal{Z} = \mathcal{Z}_1 \times \mathcal{Z}_2 \times \mathcal{Z}_3$. Assume $(D_1(Z_1, Z_2), D_2(Z_2, Z_3)) = (X_1, X_2)$ and $\mu_{Y|Z} = \delta_{D(Z)}$. Then, D satisfies $d(D_1(Z_1, Z_2), D_2(Z_2, Z_3)) = d(X_1, X_2)$ and $(X_1|X_2) = (X_1|Z_2)$ for any data fidelity function $d: \mathcal{X} \rightarrow \mathbb{R}$.*

Proof. The equation $d(D_1(Z_1, Z_2), D_2(Z_2, Z_3)) = d(X_1, X_2)$ follows directly from the assumption. Also, we have by construction that $D_1(Z_1, Z_2) \perp D_2(Z_2, Z_3)|Z_2$. This gives $(X_1|X_2) = (X_1|Z_2)$ with $X_1 = D_1(Z_1, Z_2)$ and $X_2 = D_2(Z_2, Z_3)$. \square

In general, the desired low-dimensional encoder-decoder scheme might not exist, e.g., Gaussian noise is irreducible. However, under the assumption of an optimal decoder D , we would have $(X_1|X_2 = x_2) = (D(Z_1, Z_2)|Z_2 = z_2)$ for some suitable z_2 . Theoretically, we could then sample from the conditional distribution by encoding the realized observation x_2 as (z_2, z_3) and sampling from $\mu_{Z|(Z_2, Z_3)=(z_2, z_3)}$. Again, we formalize this for clarity.

Proposition 2. *The conditions of Proposition 1 are assumed to hold. Additionally, we assume that $X = D(E(X))$ and $E(X) \sim \mu_Z = \mathcal{N}(0, I)$ with deterministic encoders $E = (E_1, E_2)$ with $E_1 : \mathcal{X}_1 \rightarrow \mathcal{Z}_1 \times \mathcal{Z}_2$ and $E_2 : \mathcal{X}_2 \rightarrow \mathcal{Z}_2 \times \mathcal{Z}_3$. Then $(X_1|X_2 = x_2) = D_1(Z_1, z_2)$ for $E_2(x_2) = (z_2, z_3)$ and $Z_1 \sim \mathcal{N}(0, I)$ holds.*

Proof. First, we note that $D(Z) = X$ by construction for $X \sim \mu_X$ and $Z \sim \mu_Z = \mathcal{N}(0, I)$. Given $X_2 = x_2$, we set $E_2(x_2) = (z_2, z_3)$. Then, we have $(X_1|X_2 = x_2) = (X_1|Z_2 = z_2)$ by Proposition 1. By design, we further know that $(X_1|Z_2 = z_2) = (D_1(Z_1, Z_2)|Z_2 = z_2)$. Since $Z \sim \mathcal{N}(0, I)$ the property $Z_1 \perp Z_2 \perp Z_3$ holds. It follows that $(X_1|X_2 = x_2) = D_1(Z_1, z_2)$ with $Z_1 \sim \mathcal{N}(0, I)$. \square

This approach models a conditional rather than just an unconditional latent Gaussian. This requires approximating both an optimal decoder and an optimal encoder that maps X to its latent representation. With $D_1(Z_1, Z_2) = D_1(Z)$ and $D_2(Z_2) = D_2(Z)$ and using the linearity of the expectation, we formulate a tractable upper bound of the Wasserstein distance using paired encoders.

Proposition 3. *Given the setting of Proposition 1 with $\tilde{Z}_1 := (Z_1, Z_2)$ and $\tilde{Z}_2 := (Z_2, Z_3)$, we define the projections $E_Z^\pi := \text{Proj}_Z(\pi)$, $E_{\tilde{Z}_1, Z_2}^\pi := \text{Proj}_{\tilde{Z}_1, Z_2}(\pi)$ and $E_{Z_2, Z_3}^\pi := \text{Proj}_{Z_2, Z_3}\pi$. Then, we have for the coupling subset $\Pi^\dagger(\mu_X, \mu_Z) := \{\pi \in \Pi(\mu_X, \mu_Z) \mid E_{\tilde{Z}_1|X}^\pi = E_{\tilde{Z}_1|X_1}^\pi, E_{\tilde{Z}_2|X}^\pi = E_{\tilde{Z}_2|X_2}^\pi\}$ the inequality*

$$\begin{aligned} W_p^p(\mu_X, \mu_Y) &= \inf_{\pi \in \Pi(\mu_X, \mu_Z)} \mathbb{E}_{\mu_X} \mathbb{E}_{E_{\tilde{Z}_1|X}^\pi} [c(X, D(Z))] \\ &\leq \inf_{\pi \in \Pi^\dagger(\mu_X, \mu_Z)} \mathbb{E}_{\mu_{X_1}} \mathbb{E}_{E_{\tilde{Z}_1|X_1}^\pi} [c(X_1, D_1(Z))] + \mathbb{E}_{\mu_{X_2}} \mathbb{E}_{E_{\tilde{Z}_2|X_2}^\pi} [c(X_2, D_2(Z))]. \end{aligned}$$

Proof. With the previous proposition we have $\Pi^\dagger(\mu_X, \mu_Z) \subset \Pi(\mu_X, \mu_Z)$ and with the linearity of our cost and expectation, we have

$$\begin{aligned} W_p^p(\mu_X, \mu_Y) &= \inf_{\pi \in \Pi(\mu_X, \mu_Z)} \mathbb{E}_{\mu_X} \mathbb{E}_{E_{\tilde{Z}_1|X}^\pi} [c(X, D(Z))] \\ &= \inf_{\pi \in \Pi(\mu_X, \mu_Z)} \mathbb{E}_{\mu_X} \mathbb{E}_{E_{\tilde{Z}_1|X}^\pi} [c(X_1, D_1(Z))] + \mathbb{E}_{\mu_X} \mathbb{E}_{E_{\tilde{Z}_1|X}^\pi} [c(X_2, D_2(Z))] \\ &\leq \inf_{\pi \in \Pi^\dagger(\mu_X, \mu_Z)} \mathbb{E}_{\mu_X} \mathbb{E}_{E_{\tilde{Z}_1|X}^\pi} [c(X_1, D_1(Z))] + \mathbb{E}_{\mu_X} \mathbb{E}_{E_{\tilde{Z}_1|X}^\pi} [c(X_2, D_2(Z))] \\ &= \inf_{\pi \in \Pi^\dagger(\mu_X, \mu_Z)} \mathbb{E}_{\mu_X} \mathbb{E}_{E_{\tilde{Z}_1|X}^\pi} [c(X_1, D_1(Z))] + \mathbb{E}_{\mu_X} \mathbb{E}_{E_{\tilde{Z}_2|X}^\pi} [c(X_2, D_2(Z))] \\ &= \inf_{\pi \in \Pi^\dagger(\mu_X, \mu_Z)} \mathbb{E}_{\mu_{X_1}} \mathbb{E}_{E_{\tilde{Z}_1|X_1}^\pi} [c(X_1, D_1(Z))] + \mathbb{E}_{\mu_{X_2}} \mathbb{E}_{E_{\tilde{Z}_2|X_2}^\pi} [c(X_2, D_2(Z))]. \end{aligned}$$

Here, we use that by construction $D_1(Z) \perp Z_3$ and $D_2(Z) \perp Z_1$. \square

We interpret the projections E_{\bullet}^{π} as (not necessarily deterministic) encoders of X into the latent space \mathcal{Z} and D_{\bullet} as a pair of decoders. A pair of optimal encoders E_{\bullet} would project the distribution μ_x onto μ_Z and optimal decoders would again project μ_Z onto $\mu_Y = \mu_X$. Practically, we are unable to ensure that $E(X) \sim \mu_Z$, but we instead optimize a relaxed version of the intractable upper Wasserstein bound from Proposition 3 similar to the original Wasserstein autoencoder.

Implementation. Now, let us assume that we have an empirical distribution of samples described by either joint distribution samples $\mu_X \approx \sum_{i=1}^n \frac{1}{n} \delta_{x_i}$ or even just by marginal samples $\mu_{X_j} \approx \sum_{i=1}^n \frac{1}{n} \delta_{(x_j)_i}$, $j = 1, 2$. Then, we can aim to find two paired encoders $E_1^{\theta}, E_2^{\theta}$ and two paired decoders $D_1^{\theta}, D_2^{\theta}$ that minimize the upper bound in Proposition 3. This allows us to create a *paired Wasserstein autoencoder*. In particular, we can sample $X \sim \mu_x$ and $Z \sim \mu_Z$ to approximate

$$\begin{aligned} \mathcal{L}(\theta) = & \mathbb{E}_{X \sim \mu_X} \left[c(A_1^{\theta}(X_1), X_1) \right] + \lambda_1 \mathbb{E}_{Z \sim \mu_Z} \text{Div}(E_1^{\theta}(X_1), \tilde{Z}_1) \\ & + \mathbb{E}_{X \sim \mu_X} \left[c(A_2^{\theta}(X_2), X_2) \right] + \lambda_1 \mathbb{E}_{Z \sim \mu_Z} \text{Div}(E_2^{\theta}(X_2), \tilde{Z}_2) \\ & + \lambda_2 \mathbb{E}_{X \sim \mu_x, Z \sim \mu_Z} [R_d(X, Z, D^{\theta}, E^{\theta})], \end{aligned}$$

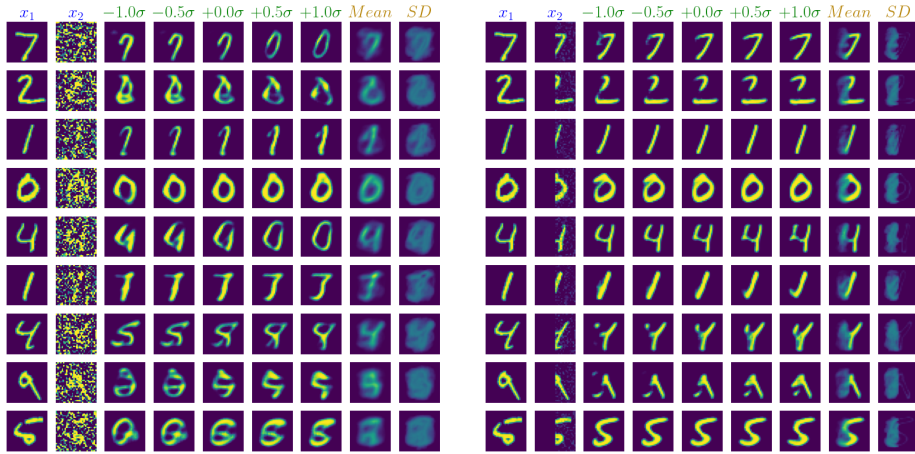
with $\tilde{Z}_1 = (Z_1, Z_2)$, $\tilde{Z}_2 = (Z_2, Z_3)$ and $A_j^{\theta} = D_j^{\theta} \circ E_j^{\theta}$, $j = 1, 2$. Note that the first two expected value terms can easily be approximated with marginal samples of μ_{X_j} , $j = 1, 2$. Here, the discrepancy term $\text{Div}(\cdot, \cdot)$ is a regularization term based on some statistical divergence to enforce $E^{\theta}(X) \stackrel{\dagger}{=} Z$. Practical options for this divergence include maximum mean discrepancies, [25], neural discriminators [25] or Wasserstein-type distances [16]. Here, we use the (entropy-regularized) squared Wasserstein-2 distance as a regularizer. As the latent reference distribution, we set $\mu_Z = \mathcal{N}(0, I)$ for all practical experiments. Lastly, we employ the additional data consistency term $R_c(X, Z, D^{\theta}, E^{\theta})$ to enforce additional knowledge about the influence of the joint distribution of X_1 and X_2 on some data fidelity function $d(\cdot)$ based on Proposition 1. This task-dependent regularizer may even enable training *without* pairs of X_1 and X_2 , i.e., training without samples from the joint distribution. We present in-depth design choices for this regularizer in the experimental section. Note that we enforce the conditional independence condition that separates $\Pi^{\dagger}(\mu_x, \mu_Z)$ from $\Pi(\mu_x, \mu_Z)$ by employing encoders $E_1^{\theta} : \mathcal{X}_1 \rightarrow \mathcal{Z}_1 \times \mathcal{Z}_2$ and $E_2^{\theta} : \mathcal{X}_2 \rightarrow \mathcal{Z}_2 \times \mathcal{Z}_3$. As a consequence, it holds $E_{\tilde{Z}_1|X}^{\theta} = E_{\tilde{Z}_1|X_1}^{\theta}$ and $E_{\tilde{Z}_2|X}^{\theta} = E_{\tilde{Z}_2|X_2}^{\theta}$ by construction. Moreover, we limit ourselves to decoders $D_1^{\theta} : \mathcal{Z}_1 \times \mathcal{Z}_2 \rightarrow \mathcal{X}_1$ and $D_2^{\theta} : \mathcal{Z}_2 \times \mathcal{Z}_3 \rightarrow \mathcal{X}_2$. This would lead to $D_1^{\theta}(E_1^{\theta}(X)) \perp \mathcal{Z}_3$ and $D_2^{\theta}(E_2^{\theta}(X)) \perp \mathcal{Z}_1$ in the case of an isotropic Gaussian latent variable $Z \sim \mathcal{N}(0, I)$. Given $X_2 = x_2$ and a paired encoder-decoder set minimizing $\mathcal{L}(\theta)$, we can approximate samples from $(X_1|X_2 = x_2)$ by simulating $D_1(Z_1, z_2)$ based on $E_2^{\theta}(x_2) = (z_2, z_3)$ and $Z_1 \sim \mathcal{N}(0, I)$. Vice versa we can simulate $(X_2|X_1 = x_1)$ using $E_1^{\theta}(x_1) = (z_1, z_2)$, $D_2(z_2, Z_3)$ and $Z_3 \sim \mathcal{N}(0, I)$.

4 Experiments

We conduct several experiments to evaluate the feasibility of conditional sampling with paired Wasserstein autoencoders³. We generally use the reconstruction loss $c(x, y) = \|x - y\|_1$ that has proven suitable for imaging tasks. This corresponds to a bound on the Wasserstein-1 distance as discussed in Proposition 3. To distinguish the different latent embeddings, we write

$$E_1^\theta = (E_1^\theta(X)_1, E_1^\theta(X)_2) \approx (Z_1, Z_2), \quad D_1^\theta(E_1^\theta(X)_1, E_2^\theta(X)_2) \approx D_1^\theta(Z_1, Z_2) \approx X_1, \\ E_2^\theta = (E_1^\theta(X)_2, E_1^\theta(X)_3) \approx (Z_2, Z_3), \quad D_2^\theta(E_2^\theta(X)_2, E_2^\theta(X)_3) \approx D_2^\theta(Z_2, Z_3) \approx X_2.$$

We evaluate the reconstruction capabilities of our approximated conditional distribution by visualizing the most likely estimation of $X_1|X_2 = x_2$ given by $D_1^\theta(0, E_2^\theta(X)_2)$. To study less likely reconstruction estimators, we depict the results of $D_1^\theta(\sigma e_j, E_2^\theta(X)_2)$ for different values of σ and some randomly chosen unit vector e_j , $j = 1, \dots, \dim(Z_1)$. Further, we display the approximation of the conditional expectation $\mathbb{E}_X[X_1|X_2 = x_2]$, i.e., $\mathbb{E}_{Z_1}[D_1^\theta(Z_1, E_2^\theta(X)_2)]$, and the pixelwise standard deviation by simulating $D_1^\theta(Z_1, E_2^\theta(X)_2)$ with $Z_1 \sim \mathcal{N}(0, I)$. Models are trained on a training dataset and evaluated on a test dataset.



(a) Denoising

(b) Inpainting

Fig. 2: Conditional sampling for denoising and image inpainting with the MNIST dataset. We aim to approximate x_1 (left, blue) based on x_2 (second from left, blue). Our most likely estimate is $+0\sigma$ and $\pm 0.5\sigma$, $\pm 1.0\sigma$ are conditional samples with decreasing likelihood (3rd-7th column, green). Lastly, we display the conditional expectation (mean) and standard deviation (SD) on the right (yellow).

³ Code will be available upon acceptance.

Denoising. An important application of conditional generative models lies in Bayesian inverse problems. Consider the relationship

$$X_2 = \text{noisy}(f(X_1)),$$

where f is a potentially ill-conditioned or non-invertible forward operator and ‘noisy’ describes a stochastic noise process. In Bayesian inverse problems, we aim to reconstruct the conditional (or posterior) distribution of X_1 given observation x_2 . Image denoising with additive noise is a classic example of an inverse problem, we use here for illustration. The inverse problem relation is described by

$$X_2 = X_1 + \varepsilon, \quad \varepsilon \sim \mathcal{N}(0, I),$$

where the forward operator is the identity. Since the noise is assumed to be Gaussian distributed, we employ the mean-square regularizer

$$R_d(X, Z, D^\theta, E^\theta) = \|X_1 - D_1^\theta(Z_1, E_2^\theta(X)_1)\|_2^2 + \|X_2 - D_2^\theta(E_1^\theta(X)_2, Z_3)\|_2^2.$$

These terms correspond to the log-likelihood under Gaussian noise. We use an encoder with four convolutional layers equipped with ReLU activation functions and batch normalization. The decoder has three convolutional upsampling layers equipped with ReLU activation functions, a sigmoidal output function, and batch normalization. The latent variables take the form $Z_j \in \mathbb{R}^{16}$, $j = 1, 2, 3$. Using the MNIST [18] data set as a canonical example, results are depicted in Fig. 2a. While expected values provide estimates of the correct digit, the conditional samples and standard deviation highlight the uncertainty due to extreme noise.

Region Inpainting. As another inverse problem example, we focus on region inpainting with the relation

$$X_2 = M \odot X_1 + \varepsilon, \quad \varepsilon \sim \mathcal{N}(0, 0.1^2 I),$$

where $M \in [0, 1]^{d_1}$ is a pre-defined inpainting mask and \odot denotes the Hadamard product. The forward operator employed in this example is non-invertible. Because of our knowledge about the forward operator, we aim to enforce data fidelity and employ the regularizer

$$R_d(X, Z, D^\theta, E^\theta) = \|M \odot X_1 - M \odot D_1^\theta(Z_1, E_2^\theta(X)_1)\|_1 + \|M \odot X_2 - M \odot D_2^\theta(E_1^\theta(X)_2, Z_3)\|_1.$$

We use the same neural network architectures as for denoising. Fig. 2b visualizes inpainting on the MNIST dataset, reconstructing the left half of each image. The expected value suggests the most likely digit, while the conditional samples and standard deviation reveal a broad range of possibilities, with high noise indicating alternative digits.

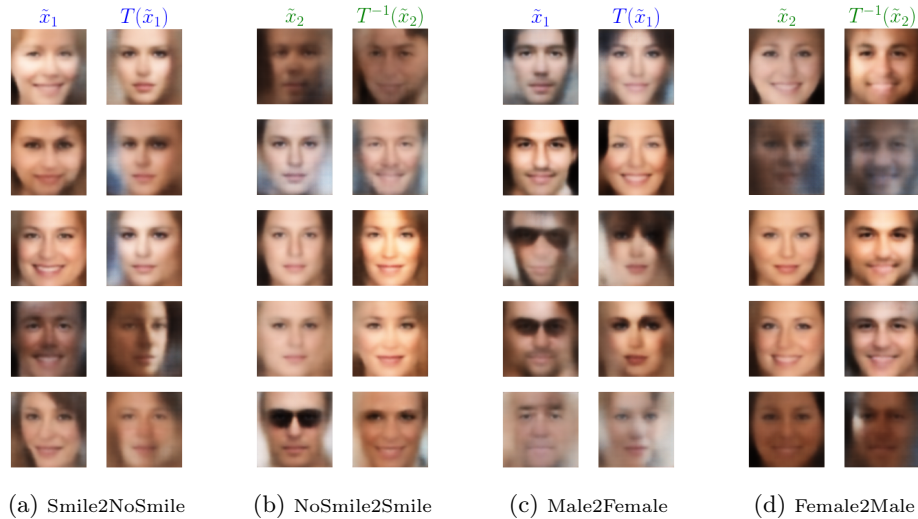


Fig. 3: Unsupervised image translation for CelebA with reconstructions \hat{x}_1, \hat{x}_2 and translated reconstructions $T(\hat{x}_1), T^{-1}(\hat{x}_2)$. We aim to translate \hat{x}_1 to $T(\hat{x}_1) := D_2(X_1(x_1))$ (blue) and \hat{x}_2 to $T^{-1}(\hat{x}_2) := D_1(X_2(x_2))$ (green). Standard autoencoder architectures produce flawed and blurry reconstructions, however.

Unsupervised Image Translation. Unsupervised image translation is another application area of conditional generative models in image processing. Here, we are given samples X_1 and X_2 from two distinct image distributions μ_1 and μ_2 in $\mathcal{P}(\mathbb{R}^d)$, and we aim to learn a conditional mapping between the two distributions, i.e., we aim to approximate the joint distribution γ of μ_1 and μ_2 . For this purpose, some assumptions about the joint distribution are necessary. The most common assumption is so-called cycle consistency. This formulates the assumption that a deterministic invertible mapping T exists between the two distributions. Formally, this can be expressed as $\gamma = (\mu_{X_1}, \mu_{X_2}) = (\mu_{X_1}, T_{\#}\mu_{X_1}) = (T_{\#}^{-1}\mu_{X_2}, \mu_{X_2})$. Indeed, any autoencoder pairs with $X_1 = D_1(E_1(X_1))$, $X_2 = D_2(E_2(X_2))$, $X_1 = D_1(Z)$, $X_2 = D_2(Z)$ and $Z = E_1(X_1) = E_2(X_2)$ suffices the cycle-consistency with $X_2 = D_2(E_1(X_1)) := T(X_1)$ and $X_1 = D_1(E_2(X_2)) := T^{-1}(X_2)$. However, cycle-consistent mappings are not unique. One suitable and unique candidate for such a map is the Monge map [17], i.e., the unique transport map with minimal squared cost. We can approximately model this map using our paired Wasserstein by setting $Z = Z_2$, omitting Z_1 and Z_3 , and employing the squared cost regularizer

$$R_d(X, Z, D^\theta, E^\theta) = \|X_1 - D_1^\theta(Z, E_2^\theta(X))\|_2^2 + \|X_2 - D_2^\theta(E_1^\theta(X))\|_2^2.$$

Due to this regularizer, the optimal solution would be the unique transport map with minimal squared cost, i.e., the Monge map. Note that the assumption of deterministic mapping implies the deterministic conditional distribution $\mu_{X_2|X_1=x_1} = \delta_{T(x_1)}$. As a result, each image is mapped to exactly another image. We use the CelebA [20] dataset for our experiments, an architecture with

5 convolutional down- and upsampling layers and latent dimension 64. Experimental results are depicted in Fig. 3. Here, we aim to translate between faces labeled as smiling and non-smiling, see Fig. 3a, 3b, and faces labeled as male and female, see Fig. 3c, 3d. Autoencoded reconstructions \hat{x}_1 and \hat{x}_2 display various artifacts due to the limitations of classic autoencoder architectures [26]. Nevertheless, comparing \hat{x}_1 with $T(\hat{x}_1)$ respectively with \hat{x}_2 with $T^{-1}(\hat{x}_2)$ we see that the model successfully translates these reconstructions.

5 Conclusion

We adapted Wasserstein autoencoders [25] to the conditional setting, addressing theoretical challenges since Wasserstein bounds on unconditional distributions do not extend to conditional ones [3]. We introduced paired Wasserstein autoencoders, mapping two inputs into a shared Gaussian latent space to enable conditional sampling. Experiments demonstrated their utility in denoising, inpainting, and unsupervised image translation, with interpretations via Monge maps from optimal transport theory. However, reconstruction artifacts from the bottleneck structure of standard autoencoders highlighted limitations, suggesting hierarchical [26] or overcomplete [5] autoencoders as a future direction. Theoretical bounds on the estimated conditional distribution remain unresolved.

Acknowledgment. M Piening acknowledges the financial support by the German Research Foundation (DFG), GRK2260 BIOQIC project 289347353. This work was partially supported by the National Science Foundation (NSF) under grant DMS-2152661 (M Chung). We thank Jannis Chemseddine, Paul Hagemann, and Gabriele Steidl (TU Berlin) for fruitful discussions.

References

1. Afkham, B., Chung, J., Chung, M.: Uncertainty quantification for goal-oriented inverse problems via variational encoder-decoder networks. *Inverse Problems* (2024)
2. Ardizzone, L., Kruse, J., Rother, C., Köthe, U.: Analyzing inverse problems with invertible neural networks. In: *Proceedings of the International Conference on Learning Representations*. OpenReview.net (2019)
3. Chemseddine, J., Hagemann, P., Wald, C., Steidl, G.: Conditional Wasserstein distances with applications in Bayesian OT flow matching. *arXiv preprint arXiv:2403.18705* (2024)
4. Chung, H., Kim, J., Mccann, M.T., Klasky, M.L., Ye, J.C.: Diffusion posterior sampling for general noisy inverse problems. In: *Proceedings of the International Conference on Learning Representations*. OpenReview.net (2023)
5. Chung, M., Archibald, R., Atzberger, P., Solomon, J.M.: Sparse l^1 -autoencoders for scientific data compression. *arXiv preprint arXiv:2405.14270* (2024)
6. Chung, M., Hart, E., Chung, J., Peters, B., Haber, E.: Paired autoencoders for likelihood-free estimation in inverse problems. *Machine Learning: Science and Technology* (2024)
7. Goodfellow, I., Pouget-Abadie, J., Mirza, M., Xu, B., Warde-Farley, D., Ozair, S., Courville, A., Bengio, Y.: Generative adversarial nets. In: *Advances in Neural Information Processing Systems*. vol. 27. Curran Associates, Inc. (2014)

8. Grathwohl, W., Chen, R.T.Q., Bettencourt, J., Duvenaud, D.: Scalable reversible generative models with free-form continuous dynamics. In: Proceedings of the International Conference on Learning Representations. OpenReview.net (2019)
9. Gu, X., Cho, K., Ha, J.W., Kim, S.: Dialogwae: Multimodal response generation with conditional Wasserstein auto-encoder. In: Proceedings of the International Conference on Learning Representations. OpenReview.net (2019)
10. Hagemann, P., Hertrich, J., Altekrüger, F., Beinert, R., Chemseddine, J., Steidl, G.: Posterior sampling based on gradient flows of the MMD with negative distance kernel. In: Proceedings of the International Conference on Learning Representations. OpenReview.net (2024)
11. Hertrich, J., Wald, C., Altekrüger, F., Hagemann, P.: Generative sliced MMD flows with Riesz kernels. In: Proceedings of the International Conference on Learning Representations. OpenReview.net (2024)
12. Ho, J., Jain, A., Abbeel, P.: Denoising diffusion probabilistic models. In: Advances in Neural Information Processing Systems. vol. 33, pp. 6840–6851. Curran Associates, Inc. (2020)
13. Huang, X., Liu, M.Y., Belongie, S., Kautz, J.: Multimodal unsupervised image-to-image translation. In: Proceedings of the European Conference on Computer Vision. Springer (2018)
14. Kim, J., Shim, B.: Generalized zero-shot learning using conditional Wasserstein autoencoder. In: Proceedings of the IEEE International Conference on Acoustics, Speech and Signal Processing. pp. 3413–3417. IEEE (2022)
15. Kim, Y.g., Lee, K., Paik, M.C.: Conditional wasserstein generator. *IEEE Transactions on Pattern Analysis and Machine Intelligence* **45**(6), 7208–7219 (2022)
16. Kolouri, S., Pope, P.E., Martin, C.E., Rohde, G.K.: Sliced Wasserstein auto-encoders. In: Proceedings of the International Conference on Learning Representations. OpenReview.net (2018)
17. Korotin, A., Selikhanovych, D., Burnaev, E.: Neural optimal transport. In: Proceedings of the International Conference on Learning Representations. OpenReview.net (2023)
18. LeCun, Y., Bottou, L., Bengio, Y., Haffner, P.: Gradient-based learning applied to document recognition. *Proceedings of the IEEE* (1998)
19. Lipman, Y., Chen, R.T., Ben-Hamu, H., Nickel, M., Le, M.: Flow matching for generative modeling. In: Proceedings of the International Conference on Learning Representations. OpenReview.net (2024)
20. Liu, Z., Luo, P., Wang, X., Tang, X.: Deep learning face attributes in the wild. In: Proceedings of the IEEE International Conference on Computer Vision. IEEE (2015)
21. Piening, M., Altekrüger, F., Hertrich, J., Hagemann, P., Walther, A., Steidl, G.: Learning from small data sets: patch-based regularizers in inverse problems for image reconstruction. *GAMM-Mitteilungen* (2024)
22. Santambrogio, F.: Optimal transport for applied mathematicians, vol. 55. Springer (2015)
23. Song, B., Kwon, S.M., Zhang, Z., Hu, X., Qu, Q., Shen, L.: Solving inverse problems with latent diffusion models via hard data consistency. In: Proceedings of the International Conference on Learning Representations. OpenReview.net (2024)
24. Stuart, A.M.: Inverse problems: a Bayesian perspective. *Acta Numerica* **19**, 451–559 (2010)
25. Tolstikhin, I., Bousquet, O., Gelly, S., Schoelkopf, B.: Wasserstein auto-encoders. In: International Conference on Learning Representations. OpenReview.net (2018)

26. Xu, W., Keshmiri, S., Wang, G.: Stacked Wasserstein autoencoder. *Neurocomputing* **363**, 195–204 (2019)